Journal of Zhejiang University-SCIENCE A (Applied Physics & Engineering)
ISSN 1673-565X (Print); ISSN 1862-1775 (Online)
www.jzus.zju.edu.cn; www.springerlink.com
E-mail: jzus@zju.edu.cn

Effective length factor of a non-symmetrical cross-bracing system with a discontinuous diagonal*

Yong CHEN[1], Yong GUO[2], Hai-wei XU[†‡1]

[1]*College of Civil Engineering and Architecture, Zhejiang University, Hangzhou 310058, China*

[2]*China Energy Engineering Group Zhejiang Electric Power Design Institute Co., Ltd., Hangzhou 310012, China*

[†]E-mail: haiwe163@163.com

Received Apr. 25, 2019; Revision accepted July 4, 2019; Crosschecked July 18, 2019

Abstract: A non-rectangular frame panel usually contains an asymmetrical cross-bracing system with interrupted diagonals, leading to a more complicated buckling behavior than a symmetrical bracing system with continuous diagonals. There have been many studies of the stability theory of symmetrical cross-bracing systems, but few related to non-symmetrical systems. In this study, we analyzed elastic out-of-plane buckling of a general non-symmetrical cross-bracing system with a discontinuous diagonal. The discontinuous and continuous diagonals have different material and geometrical properties, and are not intersected at their mid-spans. A characteristic equation is presented to compute the critical loading of a non-symmetrical cross-bracing system when the supporting diagonal is under either compression or tension. The results show that the characteristic equation of a non-symmetrical bracing system can be transformed into a form the same as that of a geometrically mono-symmetrical system. To facilitate design applications, direct closed-form empirical equations of effective length factor are established for a general non-symmetrical cross-bracing case. The validity of the proposed empirical equations was verified by comparing predicted and theoretical results, and those from a stiffness approach.

Key words: Non-symmetrical cross-bracing system; Discontinuous diagonal; Out-of-plane buckling analysis; Effective length factor

https://doi.org/10.1631/jzus.A1900169 **CLC number:** TU311.2; TU391

1 Introduction

Cross-bracing systems are widely adopted in offshore structures, transmission towers, truss structures, and industrial building walls to resist lateral loadings such as wind and earthquake actions. Generally, a cross-bracing system is in the form of an X and consists of two bracing diagonals, which are commonly subjected to compressive and tensile forces respectively, due to lateral force actions. A typical cross-bracing structure has two identical continuous diagonals which are connected at their mid-spans. However, in engineering practice, the two diagonals may have different sectional properties and lengths, and one diagonal may even be interrupted by the other (Moon et al., 2008; Davaran et al., 2015). This can lead to significantly different out-of-plane buckling behavior from a cross-bracing system with two continuous diagonals (Davaran and Hoveidae, 2009). Moreover, non-rectangular frame panels might result in geometrical asymmetry of a cross-bracing system (Thevendran and Wang, 1993), i.e. the diagonals may not connect at their mid-spans. For example, most cross-bracing systems in transmission tower structures are mono-symmetrical. Therefore, it is necessary also to consider the out-of-plane buckling

‡ Corresponding author

* Project supported by the National Natural Science Foundation of China (Nos. 51878607, 51838012, and 51508502) and the Zhejiang Provincial Natural Science Foundation of China (No. LY19E080026)

ORCID: Yong CHEN, https://orcid.org/0000-0003-0493-9536; Hai-wei XU, https://orcid.org/0000-0003-2091-5796

characteristics of a general non-symmetrical cross-bracing system with a discontinuous diagonal.

Most early studies (Dewolf and Pelliccione, 1979; El-Tayem and Goel, 1986; Kitipornchai and Finch, 1986; Picard and Beaulieu, 1987; Sabelli and Hohbach, 1999) concentrated mainly on a cross-bracing system with two identical continuous diagonals connected at their mid-spans. However, such an ideally symmetrical structure is uncommon in practical use. Thus, increasing attention has been paid to a more general case, in which the tension and compression diagonals have different geometrical and material properties (e.g. different lengths, section areas, and elastic moduli), and are connected at their respective midpoints. For such a general system, Stoman (1988) established out-of-plane buckling criteria based on the Raleigh-Ritz method of stationary potential energy. In a companion study by Stoman (1989), he extended the criteria to cases with different end constraints, and presented effective length spectra for design application. Wang and Boresi (1992) proposed a simple closed-form expression to estimate critical compression loads of a general X-bracing case with either built-in or pinned end constraints. Segal et al. (1994) presented closed-form equations for the critical load of a cross bracing incorporating the effect of the relative stiffness of the end connections and adjoining members. Considering the potential non-symmetrical characteristics of X-bracing systems in non-rectangular frame panels, Thevendran and Wang (1993) developed a numerical method to determine the critical buckling load and effective length factor of a compression diagonal based on the energy principle. Although these studies can explain the effects of diagonals with different properties on buckling behavior, they all assume that the two diagonals are continuous.

In recent years, wide use of tubular structures has led to the emergence of a large number of cross-bracing systems containing discontinuous diagonals (Chen et al., 2019). Davaran (2001) studied out-of-plane buckling loads of symmetrical X-bracing systems with intermediate connection and presented closed-form relationships for the effective length factor under either pinned or semi-rigid mid-connection. Moon et al. (2008) derived approximate solutions for elastic buckling loads of a cross-bracing system with a discontinuous diagonal and obtained effective length factors for tension and compression diagonals with different section properties and axial loads. Davaran and Hoveidae (2009) used 3D finite element models to study the effects of mid-connection detail of X-bracings comprising build-up sections on the elastic-plastic behavior of braced systems. Although these studies took discontinuous diagonals into consideration, the connection points of the two bracing diagonals were still assumed to be at their respective midpoints, which may limit their practical application.

Therefore, in this study, we considered the elastic out-of-plane buckling of a completely non-symmetrical X-bracing system with a discontinuous diagonal under a general case, i.e. continuous and discontinuous diagonals with different lengths and cross-sections, and intersection points not fixed at their mid-spans. Two load cases were analyzed: case I is non-proportional loading, under which the internal force of a bracing diagonal is assumed to be constant, and analysis focuses on the critical loading of the compression diagonal; case II is proportional loading, under which the analysis is aimed at establishing relationships between the effective length factor of the compressive diagonal and the force ratio between compressive and tensile diagonals. The intrinsic symmetry in the characteristic equation of a completely non-symmetrical cross-bracing system was revealed. For design application, direct closed-form equations are proposed for the effective length factor, and their validity is verified by theoretical solutions and numerical results obtained via a stiffness approach.

2 Non-symmetrical cross-bracing system

For a completely non-symmetrical cross-bracing system (Fig. 1), the axial tensional and compressive forces in a discontinuous compression diagonal system are denoted as T and P, respectively, while the corresponding forces in a discontinuous tension diagonal system are denoted as T' and P', respectively. The positive directions of T, P, T', and P' are shown in Fig. 1. The discontinuous diagonal consists of two members with lengths l_1 and l_2, and bending stiffness E_1I_1 and E_2I_2, respectively. The connection point divides the continuous diagonal into two parts with

bending stiffness EI, and lengths l_1' and l_2', respectively. For conservative design, it is usually assumed that both ends of the diagonals are hinged. Considering the relatively small out-of-plane bending stiffness of the connection (Davaran, 2001; Moon et al., 2008), the two members of the discontinuous diagonal are also deemed to be hinged at their intersection.

Geometrical asymmetry was considered herein by using different lengths of continuous and discontinuous diagonals, i.e. $l_1+l_2\neq l_1'+l_2'$, and setting their intersection point off their mid-spans, i.e. $l_1'\neq l_2'\neq l_1\neq l_2$ (Fig. 1). The material asymmetry was taken into account by assuming different bending stiffness of the diagonals, i.e. $E_1I_1\neq E_2I_2\neq EI$. The load asymmetry was also considered by applying unequal tension and compression forces on the diagonals, i.e. $|T|\neq|P|$ and $|T'|\neq|P'|$.

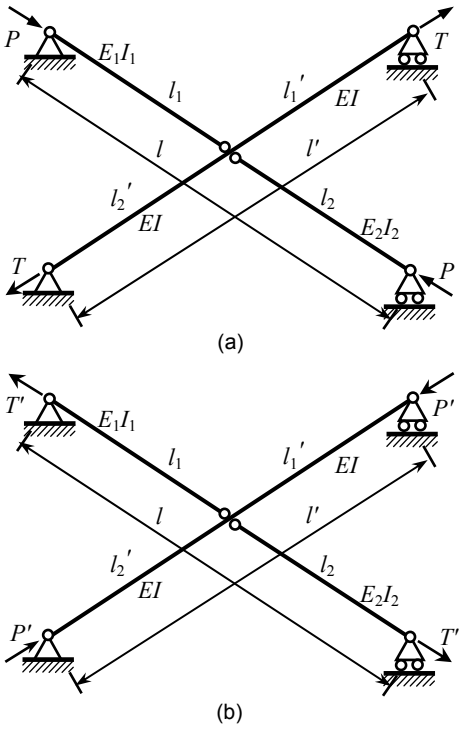

Fig. 1 Non-symmetrical cross-bracing system
(a) Discontinuous compression diagonal ($l=l_1+l_2$); (b) Discontinuous tension diagonal ($l'=l_1'+l_2'$)

3 Buckling analysis under non-proportional loading

The case of non-proportional loading herein represents constant axial forces acting on the bracing diagonals. Thus, the bracing diagonal will provide a constant lateral stiffness at the connection.

3.1 Cross-bracing system with a discontinuous tension diagonal

In the case of an X-bracing system with a discontinuous tension diagonal (Fig. 1b), the analytical model for the compressed continuous diagonal is a simply supported beam with an intermediate elastic restraint (Fig. 2). For this classic problem, extensive studies have been conducted to derive its solution (Timoshenko and Gere, 1961; Wang and Nazmul, 2003). The stiffness of the intermediate elastic support, k', provided by the discontinuous tension diagonal is

$$k'=\frac{T'}{\alpha(1-\alpha)l}, \tag{1}$$

where $\alpha=l_1/l$.

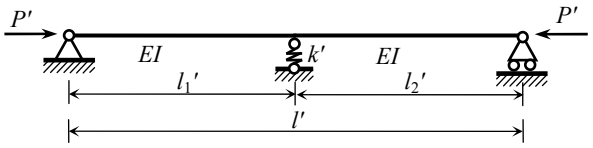

Fig. 2 Analytical model for the continuous compression diagonal

3.2 Cross-bracing system with a discontinuous compression diagonal

The case of a discontinuous compression diagonal with both hinged ends (Fig. 1a) can be modeled as two pin-connected members with a lateral elastic support at their intersection point (Fig. 3). The stiffness of the intermediate support, k, is provided by the continuous diagonal.

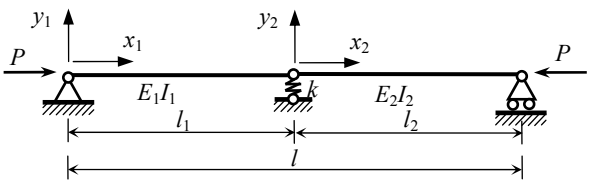

Fig. 3 Analytical model for the discontinuous compression diagonal

Based on the coordinate systems defined in Fig. 3, the governing differential equations of the compressed discontinuous diagonal are

$$E_1 I_1 \frac{\mathrm{d}^4}{\mathrm{d}x_1^4} y_1(x_1) + P \frac{\mathrm{d}^2}{\mathrm{d}x_1^2} y_1(x_1) = 0, \tag{2}$$

$$E_2 I_2 \frac{\mathrm{d}^4}{\mathrm{d}x_2^4} y_2(x_2) + P \frac{\mathrm{d}^2}{\mathrm{d}x_2^2} y_2(x_2) = 0. \tag{3}$$

Introducing non-dimensional parameters,

$$\tilde{Y}_1 = y_1 / l_1, \quad \tilde{x}_1 = x_1 / l_1, \quad \gamma_1 = \frac{P l_1^2}{E_1 I_1}, \tag{4a}$$

$$\tilde{Y}_2 = y_2 / l_2, \quad \tilde{x}_2 = x_2 / l_2, \quad \gamma_2 = \frac{P l_2^2}{E_2 I_2}, \tag{4b}$$

Eqs. (2) and (3) become

$$\frac{\mathrm{d}^4}{\mathrm{d}\tilde{x}_1^4} \tilde{Y}_1(\tilde{x}_1) + \gamma_1 \frac{\mathrm{d}^2}{\mathrm{d}\tilde{x}_1^2} \tilde{Y}_1(\tilde{x}_1) = 0, \tag{5}$$

$$\frac{\mathrm{d}^4}{\mathrm{d}\tilde{x}_2^4} \tilde{Y}_2(\tilde{x}_2) + \gamma_2 \frac{\mathrm{d}^2}{\mathrm{d}\tilde{x}_2^2} \tilde{Y}_2(\tilde{x}_2) = 0. \tag{6}$$

Thus, the non-dimensional reaction force of the intermediate support, $\tilde{R}_1$ is

$$\tilde{R}_1 = B_1^{\mathrm{d}} \tilde{Y}_1(\tilde{x}_1)\big|_{\tilde{x}_1=1}, \quad B_1^{\mathrm{d}} = \frac{l_1^3}{E_1 I_1} k, \tag{7}$$

where the stiffness k can be computed by

$$k = T\sqrt{\lambda}\sinh(\sqrt{\lambda}) \Big/ \Big\{ l' \Big[(1-\alpha')\alpha'\sqrt{\lambda}\sinh(\sqrt{\lambda}) - \sinh(\sqrt{\lambda} - \sqrt{\lambda}\alpha')\sinh(\sqrt{\lambda}\alpha') \Big] \Big\}, \tag{8}$$

where $\alpha'=l_1'/l'$ and $\lambda=Tl'^2/(EI)$. Note that Eq. (8) is also available for the case of $\lambda<0$. When taking $T=0$, Eq. (8) should be replaced by

$$k = \frac{3EI}{\alpha'^2 (1-\alpha')^2 l'^3}. \tag{9}$$

For the case of mid-span support, i.e. $\alpha'=0.5$, Eq. (8) becomes

$$k = \frac{T}{l'} \frac{4\sqrt{\lambda}}{\sqrt{\lambda} - 2\tanh(0.5\sqrt{\lambda})}. \tag{10}$$

Eq. (10) is consistent with the finding of Segal et al. (1994).

General solutions of Eqs. (5) and (6) are

$$\tilde{Y}_1(\tilde{x}_1) = C_{11} + C_{21}\tilde{x}_1 + C_{31}\sin(\sqrt{\gamma_1}\tilde{x}_1) + C_{41}\cos(\sqrt{\gamma_1}\tilde{x}_1), \tag{11}$$

$$\tilde{Y}_2(\tilde{x}_2) = C_{12} + C_{22}\tilde{x}_2 + C_{32}\sin(\sqrt{\gamma_2}\tilde{x}_2) + C_{42}\cos(\sqrt{\gamma_2}\tilde{x}_2), \tag{12}$$

where C_{ij} (i=1, 2, 3, 4; j=1, 2) are undetermined coefficients and can be derived by applying boundary conditions. Considering the continuity and force balance at the connection point, as well as the boundary conditions at both ends of the diagonals, we obtain

$$\frac{\mathrm{d}^2}{\mathrm{d}\tilde{x}_1^2} \tilde{Y}_1(0) = 0, \quad \tilde{Y}_1(0) = 0, \quad \frac{\mathrm{d}^2}{\mathrm{d}\tilde{x}_1^2} \tilde{Y}_1(1) = 0, \tag{13}$$

$$\frac{\mathrm{d}^2}{\mathrm{d}\tilde{x}_1^2} \tilde{Y}_2(0) = 0, \quad \frac{\mathrm{d}^2}{\mathrm{d}\tilde{x}_2^2} \tilde{Y}_2(1) = 0, \quad \tilde{Y}_2(1) = 0, \tag{14}$$

$$\tilde{Y}_1(\tilde{x}_1)\big|_{\tilde{x}_1=1} = \frac{1-\alpha}{\alpha} \tilde{Y}_2(\tilde{x}_2)\big|_{\tilde{x}_2=0}, \tag{15}$$

$$\frac{\mathrm{d}^3 \tilde{Y}_1}{\mathrm{d}\tilde{x}_1^3}\Big|_{\tilde{x}_1=1-\varepsilon} + \gamma_1 \frac{\mathrm{d}\tilde{Y}_1}{\mathrm{d}\tilde{x}_1}\Big|_{\tilde{x}_1=1-\varepsilon} = \frac{1}{\rho^2} \frac{\mathrm{d}^3 \tilde{Y}_2}{\mathrm{d}\tilde{x}_2^3}\Big|_{\tilde{x}_2=0+\varepsilon} + \gamma_2 \frac{1}{\rho^2} \frac{\mathrm{d}\tilde{Y}_2}{\mathrm{d}\tilde{x}_2}\Big|_{\tilde{x}_2=0+\varepsilon} + \tilde{R}_1, \tag{16}$$

where

$$\rho^2 = \frac{l_2^2}{l_1^2} \frac{E_1 I_1}{E_2 I_2}, \quad \gamma_2 = \rho^2 \gamma_1, \tag{17}$$

and ε refers to an infinitely small quantity.

Substituting Eqs. (11) and (12) into Eqs. (13)–(16) derives

$$\boldsymbol{A}\boldsymbol{C} = 0, \tag{18}$$

where $\boldsymbol{C} = \{C_{21}\ C_{31}\ C_{12}\ C_{22}\ C_{32}\ \tilde{R}_1\}^{\mathrm{T}}$ and

$$\boldsymbol{A}=\begin{bmatrix} 0 & \gamma_1\sin(\sqrt{\gamma_1}) & 0 & 0 & 0 & 0 \\ 0 & 0 & 0 & 0 & \gamma_2\sin(\sqrt{\gamma_2}) & 0 \\ 0 & 0 & 1 & 1 & 0 & 0 \\ 1 & 0 & -\dfrac{1-\alpha}{\alpha} & 0 & 0 & 0 \\ \gamma_1 & 0 & 0 & -\gamma_1 & 0 & -1 \\ B_1^{\mathrm{d}} & 0 & 0 & 0 & 0 & -1 \end{bmatrix}. \tag{19}$$

The eigenvalue equation of matrix $\boldsymbol{A}$ is thus

$$\gamma_1\gamma_2\sin(\sqrt{\gamma_1})\sin(\sqrt{\gamma_2})(\gamma_1-B_1^{\mathrm{d}}+B_1^{\mathrm{d}}\alpha)/\alpha=0. \tag{20}$$

Without loss of generality, we assume

$$0<\rho^2=\frac{l_2^2}{l_1^2}\frac{E_1I_1}{E_2I_2}<1, \tag{21}$$

which means the discontinuous diagonal member with a length of l_1 may buckle first. Thus, the minimum exact solution of Eq. (20) can be obtained by

$$\begin{cases}\gamma_1=(1-\alpha)B_1^{\mathrm{d}}, & \text{for Mode I,}\\ \gamma_1=\pi^2, & \text{for Mode II,}\end{cases} \tag{22}$$

where Modes I and II are the corresponding buckling modes which can be obtained by substituting Eq. (22) into Eq. (18). If $B_1^{\mathrm{d}}<\pi^2/(1-\alpha)$, the buckling mode is Mode I, and

$$\tilde{Y}_1(\tilde{x}_1)=C_{21}\tilde{x}_1,\quad \tilde{Y}_2(\tilde{x}_2)=\frac{\alpha}{1-\alpha}C_{21}(1-\tilde{x}_2); \tag{23}$$

if $B_1^{\mathrm{d}}>\pi^2/(1-\alpha)$, the buckling mode is Mode II, and

$$\tilde{Y}_1(\tilde{x}_1)=C_{31}\sin(\tilde{x}_1\pi),\quad \tilde{Y}_2(\tilde{x}_2)=0. \tag{24}$$

Thus, Mode II occurs when B_1^{d} is greater than the critical stiffness, $B_{\mathrm{cr}}^{\mathrm{d}}=\pi^2/(1-\alpha)$, otherwise the discontinuous diagonal will show a buckling in Mode I. Fig. 4 shows an example of two normalized buckling modes for the case of α=0.6 and ρ^2<1.

The critical buckling loads, P_{cr}, corresponding to Modes I and II can be obtained by

$$P_{\mathrm{cr}}=\begin{cases}\alpha(1-\alpha)kl, & B_1^{\mathrm{d}}<\pi^2/(1-\alpha),\\ \pi^2E_1I_1/l_1^2, & B_1^{\mathrm{d}}>\pi^2/(1-\alpha).\end{cases} \tag{25}$$

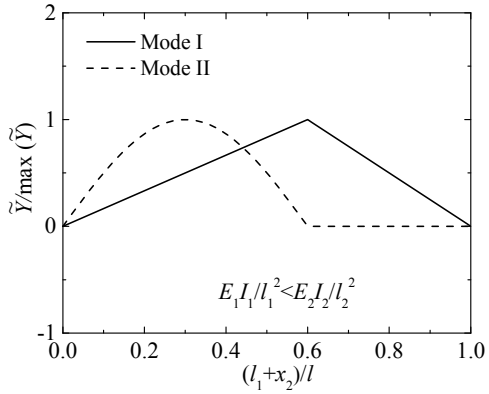

Fig. 4 Normalized buckling modes for α=0.6 and ρ^2<1

4 Buckling analysis under proportional loading

4.1 Cross-bracing system with a discontinuous compression diagonal

Defining $\psi=\dfrac{l'}{l_1}\sqrt{\dfrac{E_1I_1}{EI}}$ and $\beta=\dfrac{T}{P}$, and substituting them into Eq. (8) enables the non-dimensional stiffness, B_1^{d}, provided by the continuous diagonal to be computed by

$$\begin{aligned}B_1^{\mathrm{d}}=&\psi l_1\beta\gamma_1\sqrt{\beta\gamma_1}\sinh(\psi\sqrt{\beta\gamma_1})\\ &\Big/\Big\{l'\Big[(1-\alpha')\alpha'\psi\sqrt{\beta\gamma_1}\sinh(\psi\sqrt{\beta\gamma_1})\\ &-\sinh(\psi\sqrt{\beta\gamma_1}-\psi\sqrt{\beta\gamma_1}\alpha')\sinh(\psi\sqrt{\beta\gamma_1}\alpha')\Big]\Big\}.\end{aligned} \tag{26}$$

For the buckling in Mode I, substituting Eq. (26) into Eq. (22) yields

$$\begin{aligned}1=&\psi(1-\alpha)l_1\beta\sqrt{\beta\gamma_1}\sinh(\psi\sqrt{\beta\gamma_1})\\ &\Big/\Big\{l'\Big[(1-\alpha')\alpha'\psi\sqrt{\beta\gamma_1}\sinh(\psi\sqrt{\beta\gamma_1})\\ &-\sinh(\psi\sqrt{\beta\gamma_1}-\psi\sqrt{\beta\gamma_1}\alpha')\sinh(\psi\sqrt{\beta\gamma_1}\alpha')\Big]\Big\},\end{aligned} \tag{27}$$

where the upper-bound of γ_1 is π^2. Eq. (27) is regarded as the characteristic equation and can be used to compute the critical loading of a completely non-symmetrical cross-bracing system.

Furthermore, introducing non-dimensional parameters $\nu=\frac{l_1'(l'-l_1')}{l_1(l-l_1)}\frac{l}{l'}$, $\beta_0=\beta/\nu$, and $\psi_0^2=\psi^2\nu$, and substituting them into Eq. (27) leads to

$$\begin{aligned}1=&\psi_0\alpha'(1-\alpha')\beta_0\sqrt{\beta_0\gamma_1}\sinh(\psi_0\sqrt{\beta_0\gamma_1})\\&\Big/\Big[(1-\alpha')\alpha'\psi_0\sqrt{\beta_0\gamma_1}\sinh(\psi_0\sqrt{\beta_0\gamma_1})\\&-\sinh(\psi_0\sqrt{\beta_0\gamma_1}-\psi_0\sqrt{\beta_0\gamma_1}\alpha')\sinh(\psi_0\sqrt{\beta_0\gamma_1}\alpha')\Big].\end{aligned}\tag{28}$$

Eq. (28) has the same expression form as the characteristic equation of a geometrically mono-symmetrical cross-bracing system, which can be deduced by substituting $l_1=l_1'$ and $l=l'$ into Eq. (27). The solution of γ_1 from Eq. (28) lies in the range of $(0, \pi^2]$.

Defining $\bar{\gamma}_0=Pl^2/(EI)$, i.e. $\bar{\gamma}_0=\psi_0^2\gamma_1$, Eq. (28) can be rewritten as

$$\begin{aligned}1=&\alpha'(1-\alpha')\beta_0\sqrt{\beta_0\bar{\gamma}_0}\sinh(\sqrt{\beta_0\bar{\gamma}_0})\\&\Big/\Big[(1-\alpha')\alpha'\sqrt{\beta_0\bar{\gamma}_0}\sinh(\sqrt{\beta_0\bar{\gamma}_0})\\&-\sinh(\sqrt{\beta_0\bar{\gamma}_0}-\sqrt{\beta_0\bar{\gamma}_0}\alpha')\sinh(\sqrt{\beta_0\bar{\gamma}_0}\alpha')\Big],\end{aligned}\tag{29}$$

where $\bar{\gamma}_0\in(0,\ \psi_0^2\pi^2]$.

When $\beta_0<0$, both continuous and discontinuous diagonals are under compressive forces. However, the critical loading of a cross-bracing system is still governed by the discontinuous diagonal, because it buckles before the continuous diagonal, which means that the upper-bound of $\bar{\gamma}_0$ is obtained when the continuous diagonal buckles, i.e. $\bar{\gamma}_0=-\pi^2/\beta_0$ ($\beta_0<0$). This can be corroborated by Fig. 5 which shows the variation of $\bar{\gamma}_0$ with β_0 under different values of α' for a bracing system with $EI=E_1I_1$. All curves are below the critical curve, i.e. $\bar{\gamma}_0=-\pi^2/\beta_0$, and the buckling load of the discontinuous diagonal increases with β_0. Fig. 5 also shows that for the studied case of $EI=E_1I_1$, i.e. $\psi_0=1/\alpha'$, there is a critical value of β_0, denoted as $\beta_{0\mathrm{cr}}$ herein, beyond which $\bar{\gamma}_0$ will maintain its maximum value, i.e. $\bar{\gamma}_0=\pi^2\psi_0^2$. In this case, $\gamma_1=\pi^2$, therefore the bracing system may show a Mode II buckling according to Eq. (22).

Fig. 6 illustrates the exact theoretical solutions of $\beta_{0\mathrm{cr}}$, which are determined by substituting $\gamma_1=\pi^2$ into Eq. (28). By fitting these theoretical solutions, an empirical equation for $\beta_{0\mathrm{cr}}$ is thus obtained in the form of

$$\begin{aligned}\beta_{0\mathrm{cr}}(\alpha',\psi_0)=&-\psi_0^{-2}\alpha'^{-2}+\frac{\tanh(2\eta-2\alpha'\eta)}{\tanh(\eta)}\\&\times(0.74275\psi_0^{-2}\alpha'^{-2}+0.84866),\end{aligned}\tag{30}$$

where

$$\eta=0.35249\psi_0^2\alpha'^2+0.91226.\tag{31}$$

The values of $\beta_{0\mathrm{cr}}$ predicted by Eq. (30) are also given in Fig. 6, where ψ_0 ranges from $\sqrt{5}/5$ to $2\sqrt{2}$. Good agreement can be observed between two sets of data for bending stiffness ratios (i.e. EI/E_1I_1) ranging from 0.5 to 5 with an increment of 0.5, indicating that the proposed empirical Eq. (30) is reasonable.

Similarly, by fitting the solutions of Eq. (29) under various α', the effective length factor of the discontinuous compression brace, $K=\pi/\sqrt{\gamma_1}$, can be derived by

$$K=\begin{cases}\sqrt{\nu}\psi(\xi_1\xi_2+0.5), & \beta_0<\beta_{0\mathrm{cr}},\\ 1, & \beta_0\geq\beta_{0\mathrm{cr}},\end{cases}\tag{32}$$

where

$$\xi_1=\frac{\mu_\xi(\alpha')-0.5}{\mu_\xi(0.5)-0.5},\tag{33}$$

$$\xi_2=\begin{cases}-0.07586\bar{\beta}^4+0.31064\bar{\beta}^3-0.54441\bar{\beta}^2\\\qquad+0.91557\bar{\beta}, & \beta_0\geq-1,\\-0.0007\bar{\beta}^4+0.0153\bar{\beta}^3-0.1279\bar{\beta}^2\\\qquad+0.6999\bar{\beta}, & \beta_0<-1,\end{cases}\tag{34}$$

μ_ξ is a function of α', i.e.

$$\begin{aligned}\mu_\xi(\alpha')=&0.897\alpha'^4-1.821\alpha'^3+0.617\alpha'^2\\&+0.300\alpha'+2.836,\end{aligned}\tag{35}$$

and $\bar{\beta}$ can be computed by

$$\overline{\beta} = 8.593 - \frac{8.593}{\mu_\beta(\alpha') + 8}(\beta_0 + 8), \tag{36}$$

where

$$\mu_\beta(\alpha') = -7.29\alpha'^4 + 12.94\alpha'^3 - 9.89\alpha'^2 + 3.79\alpha' + 0.01. \tag{37}$$

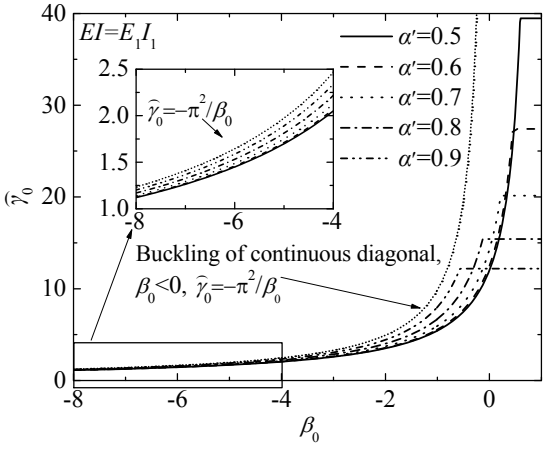

Fig. 5 Variation of $\hat{\gamma}_0$ with β_0 for $EI=E_1I_1$

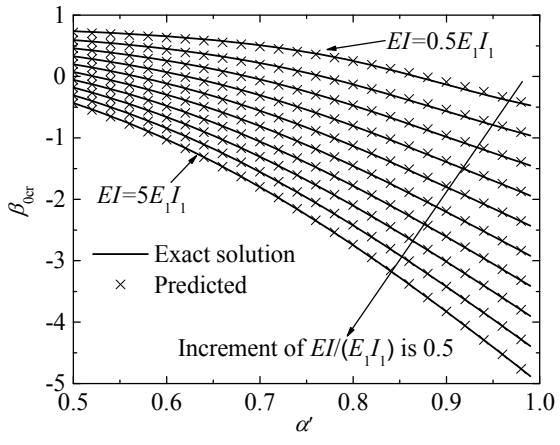

Fig. 6 Variation of β_{0cr} with α'

For a geometrically mono-symmetrical cross-bracing system with a discontinuous diagonal, we have $l_1=l_1'$ and $l=l'$, which leads to $\nu=1.0$, $\psi=\psi_0$, and $\beta=\beta_0$. Fig. 7 compares predicted effective length factors based on the empirical Eq. (32) with the exact solutions obtained from the original Eq. (29) under four different bending stiffness ratios. The prediction results matched well with exact solutions for all calculated cases.

4.2 Cross-bracing system with a discontinuous tension diagonal

For a cross-bracing system with a discontinuous tension diagonal, the continuous diagonal is under compression, while the discontinuous diagonal is subjected to tension (Fig. 1b). Eq. (27) is still available for the cases of $P=-T'\le 0$ and $T=-P'\le 0$. Defining $\gamma'=P'l'^2/(EI)$ derives $\gamma'=-\beta\psi^2\gamma_1$. The corresponding effective length factor of the continuous compression diagonal is $K'=\pi/\sqrt{\gamma'}$. Since T' is larger than 0 in this case, we conclude that $\gamma'_\infty>\gamma'\ge\pi^2$, where γ'_∞ corresponds to the case of $T'\to\infty$. This implies $\gamma'_\infty=P'_{cr}l'^2/(EI)$, where P'_{cr} is the critical loading of a two-span continuous beam subjected to axial compression force. Therefore, the relationship between γ'_∞ and α' can be derived by

$$0=(\alpha'-\alpha'^2)\sqrt{\gamma'_\infty}\sin(\sqrt{\gamma'_\infty}) + \sin(\sqrt{\gamma'_\infty}\alpha'-\sqrt{\gamma'_\infty})\sin(\sqrt{\gamma'_\infty}\alpha'), \tag{38}$$

where γ'_∞ can be approximated by

$$\sqrt{\gamma'_\infty} \approx -90.86(1-\alpha')^4+91.97(1-\alpha')^3 - 32.99(1-\alpha')^2 + 9.276(1-\alpha') + 4.074, \tag{39}$$

where $0.5\le\alpha'\le 1$. For a cross-bracing system with a discontinuous tension diagonal, the critical loading can be obtained by solving Eq. (28), where $\beta=P'/T'>0$ and the solution domain of γ_1 is $\left(-\gamma'_\infty\frac{1}{\beta\psi^2}, -\frac{\pi^2}{\beta\psi^2}\right]$. Using an imaginary number description, Eq. (27) can be rewritten in terms of γ', i.e.

$$1=(1-\alpha)l_1\beta\sqrt{\gamma'}\sin(\sqrt{\gamma'}) \Big/\left\{l'\left[(1-\alpha')\alpha'\sqrt{\gamma'}\sin(\sqrt{\gamma'}) - \sin(\sqrt{\gamma'}-\sqrt{\gamma'}\alpha')\sin(\sqrt{\gamma'}\alpha')\right]\right\}. \tag{40}$$

substituting ν and β_0 into Eq. (40) yields

$$\frac{\nu}{\beta}=\alpha'(1-\alpha')\sqrt{\gamma'}\sin(\sqrt{\gamma'}) \Big/\left[\alpha'(1-\alpha')\sqrt{\gamma'}\sin(\sqrt{\gamma'}) - \sin(\sqrt{\gamma'}-\sqrt{\gamma'}\alpha')\sin(\sqrt{\gamma'}\alpha')\right], \tag{41}$$

where γ' lies in the range of $[\pi^2, \gamma'_\infty)$.

For $\alpha' \geq 0.5$, by fitting the exact solutions obtained from $K' = \pi/\sqrt{\gamma'}$, the relationship between the effective length factor, K', and $\beta'=T'/P'$ can be estimated by

$$K'=\begin{cases}\dfrac{1}{1+\kappa(\nu\beta'-1)^{\chi}}\left(\alpha'-\dfrac{\pi}{\sqrt{\gamma'_\infty}}\right)+\dfrac{\pi}{\sqrt{\gamma'_\infty}}, & \nu\beta'>1,\\ 1-\nu\beta'+\nu\beta'\alpha', & \nu\beta'\leq 1,\end{cases} \tag{42}$$

where

$$\kappa=(-8.1004+37.6598\alpha'-59.7324\alpha'^2+33.4999\alpha'^3)^{-1}, \tag{43}$$

and

$$\chi=0.8472+0.4438\alpha'. \tag{44}$$

5 Verification via a stiffness approach

Applying a stiffness approach to out-of-plane buckling analysis, we have

$$\boldsymbol{KX} = \boldsymbol{F}, \tag{45}$$

where $\boldsymbol{F}$ is the vector of disturbance forces, $\boldsymbol{X}$ is the vector of out-of-plane displacements, and $\boldsymbol{K}$ is the out-of-plane stiffness matrix which can be determined from,

$$\boldsymbol{K} = \boldsymbol{K}_{\mathrm{B0}} + \boldsymbol{K}_{\mathrm{T0}} + \boldsymbol{K}_{\mathrm{B1}} + \boldsymbol{K}_{\mathrm{T1}} + \boldsymbol{K}_{\mathrm{B2}} + \boldsymbol{K}_{\mathrm{T2}}, \tag{46}$$

where the subscript 'B' represents the stiffness caused by bending deflection, and the subscript 'T' represents the stiffness caused by axial tension deflection.

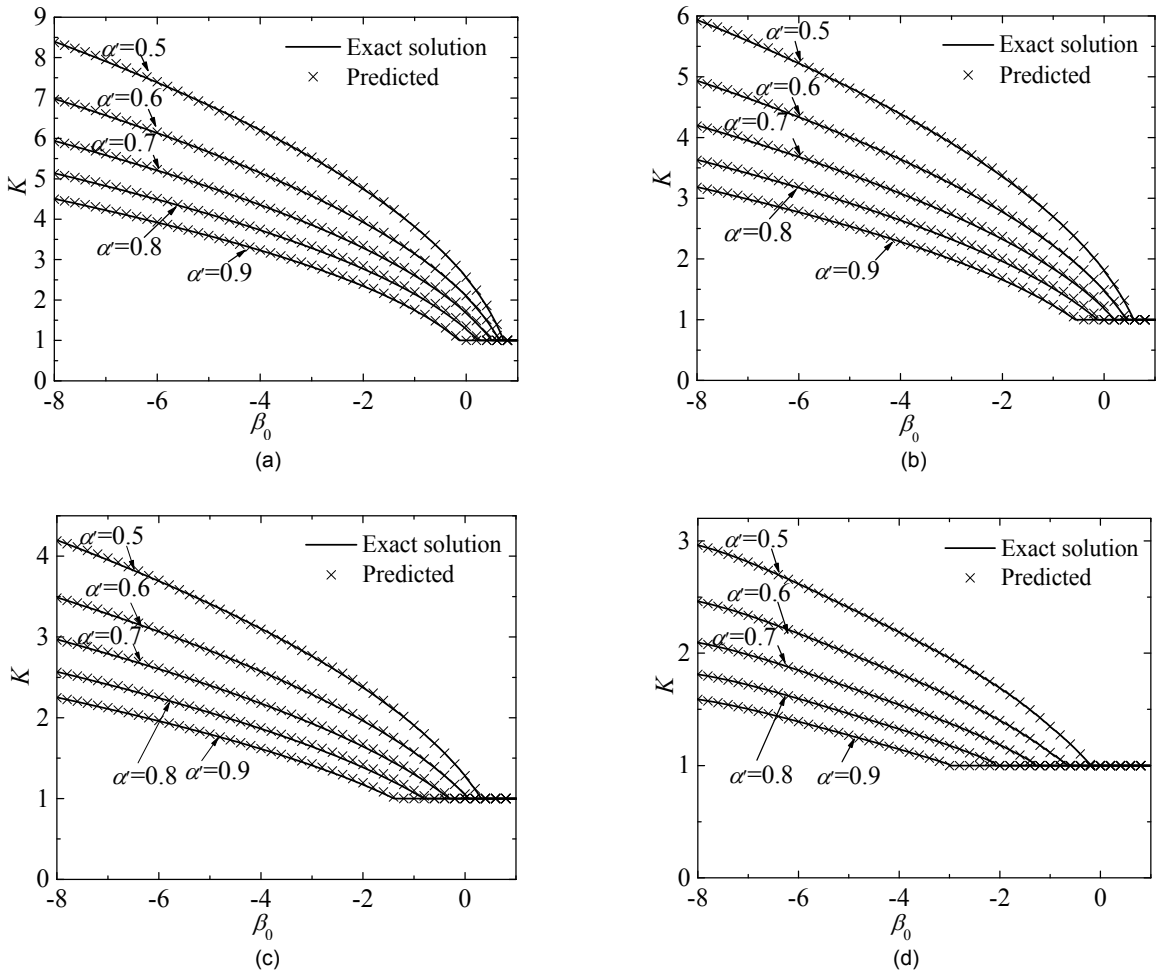

Fig. 7 Comparison between predicted and exact solutions of effective length factor
(a) $EI=0.5E_1I_1$; (b) $EI=E_1I_1$; (c) $EI=2E_1I_1$; (d) $EI=4E_1I_1$

The subscript '0' represents the continuous diagonal, whereas subscripts '1' and '2' represent members of a discontinuous diagonal with lengths l_1 and l_2, respectively. The out-of-plane stiffness matrix can be obtained via finite element method. Further details can be found in (Chen et al., 2015).

5.1 Cross-bracing systems with a discontinuous compression diagonal

According to Fig. 1a, the stiffness matrix is

$$\boldsymbol{K}=\sum_{i=0}^{2}\boldsymbol{K}_{\mathrm{B}i}-P(\boldsymbol{k}_{\mathrm{T1}}+\boldsymbol{k}_{\mathrm{T2}}-\beta\boldsymbol{k}_{\mathrm{T0}}), \tag{47}$$

where $\boldsymbol{k}$ represents the stiffness matrix caused by unit axial force. In this case, the out-of-plane buckling of the cross-bracing system requires

$$\left|\left(\sum_{i=0}^{2}\boldsymbol{K}_{\mathrm{B}i}\right)^{-1}(\boldsymbol{k}_{\mathrm{T1}}+\boldsymbol{k}_{\mathrm{T2}}-\beta\boldsymbol{k}_{\mathrm{T0}})-\frac{1}{P}\right|=0. \tag{48}$$

The minimum solution of P in Eq. (48) is the critical loading of the cross-bracing system.

5.2 Cross-bracing systems with a discontinuous tension diagonal

According to Fig. 1b, a similar stiffness matrix can be derived:

$$\boldsymbol{K}=\sum_{i=0}^{2}\boldsymbol{K}_{\mathrm{B}i}-P'(-\beta'\boldsymbol{k}_{\mathrm{T1}}-\beta'\boldsymbol{k}_{\mathrm{T2}}+\boldsymbol{k}_{\mathrm{T0}}). \tag{49}$$

Similarly, the out-of-plane buckling of the cross-bracing system in this case requires

$$\left|\left(\sum_{i=0}^{2}\boldsymbol{K}_{\mathrm{B}i}\right)^{-1}(-\beta'\boldsymbol{k}_{\mathrm{T1}}-\beta'\boldsymbol{k}_{\mathrm{T2}}+\boldsymbol{k}_{\mathrm{T0}})-\frac{1}{P'}\right|=0. \tag{50}$$

The minimum solution of P' in Eq. (50) is thereby the critical loading of the cross-bracing system.

5.3 Case study

Assuming a completely non-symmetrical system with $l_1'=0.7l'$, $l_2'=0.3l'$, $l_1=0.4l$, $l_2=0.6l$, $l=0.8l'$, $E_1I_1=0.5EI$, and $E_2I_2=2EI$, leads to $\nu=1.0938$ and $\psi=2.21$. First, we study the case of a discontinuous diagonal subjected to compression. Since $\rho^2=0.563<1$, the critical loading of the compressed diagonal will be controlled by the member with a length of l_1 and flexural rigidity of E_1I_1. Variation of K with T/P predicted using empirical Eq. (32), along with the corresponding results via the stiffness approach is shown in Fig. 8a. Good agreement can be observed between the two methods.

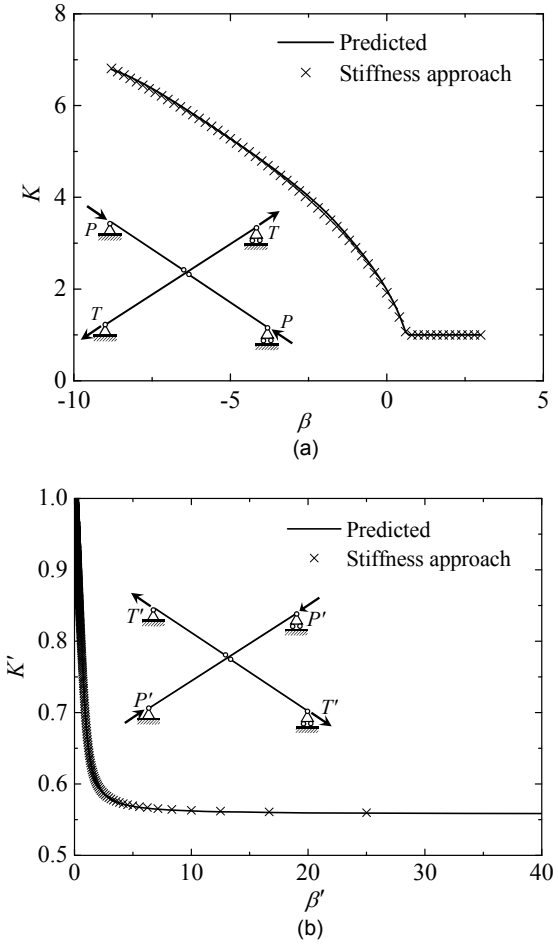

Fig. 8 Comparison of effective length factors
(a) Discontinuous compression diagonal; (b) Discontinuous tension diagonal

Consider the case of a discontinuous diagonal subjected to tension forces while the continuous diagonal is under compression. In this case, the continuous diagonal with length l' and flexural rigidity EI is considered for estimating the critical loading. Similarly, Fig. 8b illustrates the values of K' calculated from Eq. (42) along with their corresponding numerical results via the stiffness approach. Eq. (42) can

give reasonable predictions of K', which match well with their numerical counterparts.

In a case adopted by Davaran (2001), two identical diagonals were used, and the connection of the diagonals was at their midpoints, which implied $l_1'=0.5l'$, $l_2'=0.5l'$, $l_1=0.5l$, $l_2=0.5l$, $l=l'$, $E_1I_1=EI$, and $E_2I_2=EI$. Thus, $\nu=1.0$, $\psi=2.0$, and $\rho^2=1.0$ can be obtained. Fig. 9 compares the effective length factors from Davaran (2001) with those obtained from empirical equations (i.e. Eqs. (32) and (42)), and by the stiffness approach, respectively. There is a good agreement between the three sets of data, suggesting that the proposed empirical equations of the effective length factor are reliable.

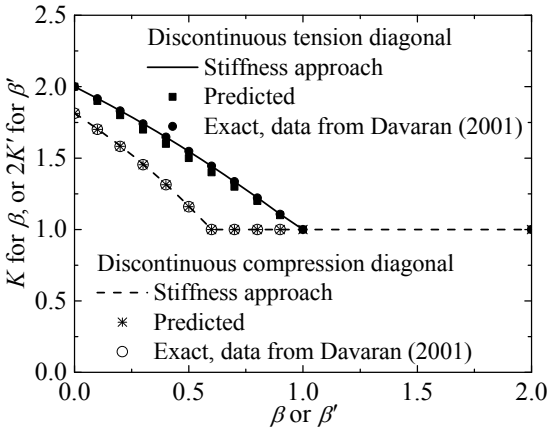

Fig. 9 Comparison of effective length factors

6 Conclusions

Elastic out-of-plane buckling analysis was performed on a completely non-symmetrical cross-bracing system with a discontinuous diagonal. The main conclusions are:

1. By using variable substitution, the presented characteristic equation (i.e. Eq. (27)) of a completely non-symmetrical cross-bracing system could be transformed into an expression (i.e. Eq. (28)) having the same form as the characteristic equation of a geometrically mono-symmetrical system. The proposed characteristic equation can be used to evaluate the critical loading of a cross-bracing system whether the supporting diagonal is under compression or tension.

2. When the discontinuous and continuous diagonals are both under compression, the discontinuous diagonal may buckle before the continuous diagonal and is thereby the control case in determining critical loading of a cross-bracing system. There is a critical ratio of tension to compression (i.e. T/P) beyond which one of the discontinuous diagonal members will buckle first.

3. The out-of-plane buckling of the discontinuous compression diagonal will show a pure sway mode (no bending deformation), on condition that (1) the non-dimensional stiffness B_1^{d} from the supporting continuous diagonal is less than a critical value of $\pi^2/(1-\alpha)$, in the case of non-proportional loading, or (2) the ratio of tension to compression, i.e. T/P, is less than a critical value, $\nu\beta_{0\mathrm{cr}}$, in the case of proportional loading.

4. For design purposes, direct closed-form equations of the effective length factor were formulated for a general cross-bracing system in which the tension and compression diagonals have different material and geometry properties, and the intersection point of diagonals is not at their midpoints. By comparing the prediction results with corresponding theoretical solutions, the validity of the presented empirical equations was verified for cases of $2\sqrt{2}\geq\psi_0\geq\sqrt{5}/5$, $\beta_0\geq-8$, $\beta'\geq0$, $0.9\geq\alpha'\geq0.5$, and $\rho^2\leq1.0$. Case studies showed that the predicted results via empirical equations agreed well with those obtained from a stiffness approach and those from the literature. The proposed effective length factor for the discontinuous compression diagonal is applied to the partial length of the diagonal, whereas that for the continuous compression diagonal is applied to the full length of the diagonal.

Contributors

Conceptualization, Yong CHEN and Yong GUO; Methodology, Hai-wei XU; Formal analysis and validation, Hai-wei XU; Funding acquisition, Yong CHEN and Hai-wei XU; Writing of original draft, Yong CHEN; Review and editing, Hai-wei XU.

Conflict of interest

Yong CHEN, Yong GUO, and Hai-wei XU declare that they have no conflict of interest.

References

Chen Y, McFarland DM, Spencer Jr BF, et al., 2015. Exact solution of free vibration of a uniform tensioned beam combined with both lateral and rotational linear

sub-systems. *Journal of Sound and Vibration*, 341:206-221. https://doi.org/10.1016/j.jsv.2014.12.013

Chen Y, Hu ZZ, Guo Y, et al., 2019. Ultimate bearing capacity of CHS X-joints stiffened with external ring stiffeners and gusset plates subjected to brace compression. *Engineering Structures*, 181:76-88. https://doi.org/10.1016/j.engstruct.2018.12.005

Davaran A, 2001. Effective length factor for discontinuous X-bracing systems. *Journal of Engineering Mechanics*, 127(2):106-112. https://doi.org/10.1061/(asce)0733-9399(2001)127:2(106)

Davaran A, Hoveidae N, 2009. Effect of mid-connection detail on the behavior of X-bracing systems. *Journal of Constructional Steel Research*, 65(4):985-990. https://doi.org/10.1016/j.jcsr.2008.11.005

Davaran A, Gélinas A, Tremblay R, 2015. Inelastic buckling analysis of steel X-bracing with bolted single shear lap connections. *Journal of Structural Engineering*, 141(8): 04014204. https://doi.org/10.1061/(asce)st.1943-541x.0001141

Dewolf JT, Pelliccione JF, 1979. Cross-bracing design. *Journal of the Structural Division*, 105(7):1379-1391.

El-Tayem AA, Goel SC, 1986. Effective length factor for the design of X-bracing systems. *Engineering Journal*, 23(1): 41-45.

Kitipornchai S, Finch DL, 1986. Stiffness requirements for cross bracing. *Journal of Structural Engineering*, 112(12):2702-2707. https://doi.org/10.1061/(asce)0733-9445(1986)112:12(2702)

Moon J, Yoon KY, Han TS, et al., 2008. Out-of-plane buckling and design of X-bracing systems with discontinuous diagonals. *Journal of Constructional Steel Research*, 64(3): 285-294. https://doi.org/10.1016/j.jcsr.2007.07.008

Picard A, Beaulieu D, 1987. Design of diagonal cross bracings. Part 1: theoretical study. *Engineering Journal*, 24(3):122-126.

Sabelli R, Hohbach D, 1999. Design of cross-braced frames for predictable buckling behavior. *Journal of Structural Engineering*, 125(2):163-168. https://doi.org/10.1061/(asce)0733-9445(1999)125:2(163)

Segal F, Levy R, Rutenberg A, 1994. Design of imperfect cross-bracings. *Journal of Engineering Mechanics*, 120(5):1057-1075. https://doi.org/10.1061/(asce)0733-9399(1994)120:5(1057)

Stoman SH, 1988. Stability criteria for X-bracing systems. *Journal of Engineering Mechanics*, 114(8):1426-1434. https://doi.org/10.1061/(asce)0733-9399(1988)114:8(1426)

Stoman SH, 1989. Effective length spectra for cross bracings. *Journal of Structural Engineering*, 115(12):3112-3122. https://doi.org/10.1061/(asce)0733-9445(1989)115:12(3112)

Thevendran V, Wang CM, 1993. Stability of nonsymmetric cross-bracing systems. *Journal of Structural Engineering*, 119(1):169-180. https://doi.org/10.1061/(asce)0733-9445(1993)119:1(169)

Timoshenko SP, Gere JM, 1961. Theory of Elastic Stability. McGraw-Hill, New York, USA.

Wang CM, Nazmul IM, 2003. Buckling of columns with intermediate elastic restraint. *Journal of Engineering Mechanics*, 129(2):241-244. https://doi.org/10.1061/(asce)0733-9399(2003)129:2(241)

Wang DQ, Boresi AP, 1992. Theoretical study of stability criteria for X-bracing systems. *Journal of Engineering Mechanics*, 118(7):1357-1364. https://doi.org/10.1061/(asce)0733-9399(1992)118:7(1357)

中文概要

题　目： 含非连续支撑的非对称交叉斜撑体系的计算长度系数

目　的： 非矩形平面框架致使其交叉斜撑体系具有非对称性，而采用了非连续支撑的非对称非连续交叉支撑体系的面外稳定问题更为复杂。本文旨在通过建立无量纲稳定特征方程，从理论上深入阐释该交叉支撑体系的面外屈曲特征，并为工程设计提供显式的压杆计算长度系数的计算公式。

创新点： 1. 建立一般情况下非对称非连续交叉斜撑体系的无量纲特征方程；2. 针对各种可能受力工况，详细分析该交叉支撑体系的面外屈曲特征，并给出理论解释；3. 提出非对称非连续交叉斜撑体系中压杆计算长度系数的显式经验计算公式。

方　法： 1. 通过对非对称非连续交叉支撑体系进行弹性面外屈曲建模，以及稳定平衡方程的无量纲化，推导出其相应的特征方程；2. 通过变量替换，揭示其内在对称性，从而为经验公式的构造提供依据；3. 针对各种受力工况，进行求解域分析和确定，完成特征方程的求解，以进行面外屈曲特征分析，并提出压杆计算长度系数的经验公式；4. 利用经验公式对多个实例进行计算，并与基于有限元的刚度法结果以及以往的文献数据进行比较，以验证经验公式的可靠性。

结　论： 1. 推导出了非对称非连续交叉斜撑体系的特征方程；采用无量纲参数后，该方程具有一般性。2. 通过变量替换，该方程可以转换为与单轴几何对称交叉斜撑相同的特征方程形式。3. 当交叉斜撑中的连续杆和非连续杆同时受压时，非连续杆将率先失稳。4. 针对各种受力工况，提出了交叉支撑体系的压杆计算长度系数的显式经验公式，且计算结果兼具可靠性和准确性。

关键词： 非对称交叉支撑体系；非连续支撑；面外屈曲分析；计算长度系数